

# Modeling heat and mass transfer in laminar forced convection in a vertical channel: influence of Reynolds number

## ABSTRACT

The phenomena of heat and mass transfer are of considerable interest in the field of energy. We present in this work a numerical study of the heat and mass transfers in laminar forced convection in a vertical channel, whose wet walls interact with the external environment. Based on simplifying assumptions, the flow, whose thermo-physical properties depend on temperature and relative humidity, was modelled by the Navier-Stokes equations and the flow conservation equation. The finite volume method was used to discretize the equations and the resulting algebraic equation systems were solved using Thomas' and Gauss' algorithms. The influence of the Reynolds number on thermal and mass transfers was mainly investigated. Numerical simulations with Reynolds numbers of 500, 1000 and 1500 have allowed a detailed study of the flow structure as well as thermal and mass fields. The numerical results obtained, presented in isotherms, iso-concentrations, Sherwood and Nusselt numbers, reveal the important role of the Reynolds number in heat and mass transfers in a vertical channel. The rates of these transfers at the entrance to the channel differ from those at the exit.

*Keywords: Laminar forced convection, heat and mass transfer, Reynolds number, vertical channel.*

## 1. INTRODUCTION

In the last two decades, convection heat transfers have been widely investigated due to their diverse applications. Of the two types of convection, forced convection and natural convection, forced convection remains the one that keeps attention in studies [1][2][3]. Nowadays the interest of heat and mass transfer studies within cavities is dictated by its importance in applications such as drying-smoking, thermal building, cooling of electronic components, nuclear reactors, fire engineering, thermal desalination of sea water, and more [4][5][6]. Several parameters such as the nature of the fluid, its speed, its relative humidity and its inlet temperature, the temperature of the walls, make the flow in the channels complex. They have therefore been the subject of numerous works, both numerical and experimental. O. Mechergui [6], who studied the phenomenon of evaporation in laminar flow in his thesis, demonstrated the influence of parameters such as wall temperature, heat flux density, temperature and humidity at the channel inlet on the velocity, concentration and temperature profiles inside the channel for heat and mass transfer. To demonstrate the dependence of the physical properties of moist air on both temperature and water vapor concentration, Oulaidet *al.* [7] considered a warm air stream whose physical properties are initially constant, and then variable. As the difference between the results of the two models was significant (between 8 and 30%) for all hydrodynamic, thermal and mass quantities, they concluded that it was important to consider the variability of thermo-physical properties in the mathematical model. Given the importance of parameters such as velocity, temperature and

humidity, some authors have focused on their effects on heat and mass transfer. Thus, Karim *et al.* [8] conducted a numerical study of forced convection heat and mass transfers in a straight triangular cavity with adiabatic and mobile wall. To show the importance of inertial forces, the authors focused on the impacts of different Reynolds numbers between 50 and 200 on heat and mass transfers during forced convection flow. Their results show that an increase in the Reynolds number improves the heat transfer. Some authors have used the Reynolds number for other applications. Singh *et al.* [9] studied the impact of a small number of Reynolds on the probe coefficient at different angles of the pitot tube type S. Azizi *et al.* [10] Digitally studied the effects of thermal and buoyancy forces on air flows in a vertical channel made up of parallel plates. These plates are wetted by a thin film of liquid water and maintained at a constant temperature lower than the air entering the channel. The authors show that buoyancy forces have a significant effect on coupled heat and material transfers. The latent heat transfer may be more or less important compared to the sensitive heat transfer. The extent of these transfers depends on temperature and humidity conditions. Boukadida *et al.* [11] studied the effect of control parameters on air velocity, temperature and humidity inside a horizontal channel. Their results showed that air temperature, longitudinal velocity and water vapor concentration increased from the inlet to the outlet of the channel. Helel *et al.* [12] revealed, after a numerical study of heat and mass transfer mechanisms in laminar flow, that these transfers are greater in the vicinity of the leading edge than at the outlet. A numerical study carried out by N. Galanis *et al.* [13] on mixed laminar convection with phase change between two parallel flat plates wetted with a liquid film of water at a constant temperature lower than that of air at the channel inlet, revealed that the ratio between the latent and sensible Nusselt number is seven at the channel inlet, whereas it is three at the outlet. Inside the channel, Lin *et al.* [14], who studied the combined effects of buoyancy, thermal and mass diffusion on heat transfer by laminar forced convection, showed that heat transfer in the flow is dominated by latent mode transport, with the ratio of latent to sensible heat flux having a minimum for a fixed parietal temperature. The effect of flow velocity on heat transfer has been studied by Yan *et al.* [15]. In a typical study of coupled heat and mass transfer along a heated plate, in addition to the importance of latent heat transport, the authors showed that parietal temperature decreases with increasing flow velocity. Mezaache and Daguene [16] have numerically examined the evaporation, in a forced flow of humid air, of a thin film of water trickling over an inclined flat plate, considered adiabatic or traversed by a constant heat flux. They have shown that the effect of flow velocity is an important parameter, and that heat transfer is dominated by that associated with the liquid-vapor transition. Cherif *et al.* [17] [18] presented the results of an experimental and numerical study of coupled heat and mass transfer in a vertical channel. Evaporated mass flux and thermal efficiency are calculated for different heat flux densities and flow velocities. They revealed that evaporation takes place over the majority of the wall surface and, in some cases, evaporative cooling occurs particularly for low heat flux and high air velocities. Turki *et al.* [19] have shown that the contribution of forced convection to heat transfer is greater than that of mixed convection. The literature results show that the influence of the Reynolds number on thermal and mass transfers within the channels has not been sufficiently investigated. This number serves as a bridge between the theoretical and practical realms of fluid dynamics, and its relatively small values are of paramount importance in micro-fluidics. Our main objective is to study the influence of Reynolds number on unsteady laminar forced convection flow in a vertical channel where the thermo-physical properties of the fluid depend on temperature and humidity. Specifically, we will analyze the effects of Reynolds numbers of 500, 1000 and 1500 on the temperature, mass and velocity fields.



$$\frac{\partial(\rho V)}{\partial x} + \frac{\partial(\rho U)}{\partial z} = 0 \quad (1)$$

❖ **The axial equation of momentum**

$$\rho \frac{\partial U}{\partial t} + \frac{\partial(\rho VU)}{\partial x} + \frac{\partial(\rho UU)}{\partial z} = -\frac{\partial P}{\partial z} + \frac{\partial}{\partial x} \left( \mu \frac{\partial U}{\partial x} \right) + \frac{\partial}{\partial z} \left( \mu \frac{\partial U}{\partial z} \right) \quad (2)$$

❖ **The radial equation of momentum**

$$\rho \frac{\partial V}{\partial t} + \frac{\partial(\rho VV)}{\partial x} + \frac{\partial(\rho UV)}{\partial z} = \frac{\partial}{\partial x} \left( \mu \frac{\partial V}{\partial x} \right) + \frac{\partial}{\partial z} \left( \mu \frac{\partial V}{\partial z} \right) \quad (3)$$

❖ **The energy conservation equation**

$$\rho C_p \frac{\partial T}{\partial t} + \frac{\partial(\rho C_p VT)}{\partial x} + \frac{\partial(\rho C_p UT)}{\partial z} = \frac{\partial}{\partial x} \left( \lambda \frac{\partial T}{\partial x} \right) + \frac{\partial}{\partial z} \left( \lambda \frac{\partial T}{\partial z} \right) \quad (4)$$

❖ **The water vapor diffusion equation**

$$\rho \frac{\partial C}{\partial t} + \frac{\partial(\rho VC)}{\partial x} + \frac{\partial(\rho UC)}{\partial z} = \frac{\partial}{\partial x} \left( \rho D \frac{\partial C}{\partial x} \right) + \frac{\partial}{\partial z} \left( \rho D \frac{\partial C}{\partial z} \right) \quad (5)$$

❖ **The flow rate conservation equation**

$$\int_0^R U dx = Q_{ev} + Q_e \quad (6)$$

**2.2.3. INITIAL CONDITIONS**

$$U(x, z) = 0 ; V(x, z) = 0 ; C(x, z) = C_e ; T(x, z) = T_e \quad (7a-d)$$

**2.2.4. BOUNDARY CONDITIONS**

- At the channel entrance:  $z = 0; 0 \leq x \leq R$

$$U(x, z) = \frac{3}{2} U_e \left[ 1 - \left( \frac{x}{R} \right)^2 \right] \quad (8)$$

$$V(x, z) = 0 ; C(x, z) = C_e ; T(x, z) = T_e \quad (9a-c)$$

- At the channel outlet:  $z = H; 0 \leq x \leq R$

$$\frac{\partial U(x, z)}{\partial z} = 0 ; \frac{\partial V(x, z)}{\partial z} = 0 ; \frac{\partial T(x, z)}{\partial z} = 0 ; \frac{\partial C(x, z)}{\partial z} = 0 \quad (10a-d)$$

- At the axis of symmetry:  $x = 0; 0 \leq z \leq H$

$$V(x, z) = 0 \quad (11)$$

$$\frac{\partial U(x, z)}{\partial x} = 0 ; \frac{\partial T(x, z)}{\partial x} = 0 ; \frac{\partial C(x, z)}{\partial x} = 0 \quad (12a-c)$$

- To the wall:  $x = R; 0 \leq z \leq H$

$$U(x, z) = 0 \quad (13)$$

$V(x, z) = V_{ev}$  (14)  
 $V_{ev}$ : is the evaporation rate at the wall. Its calculation is detailed in the work of Eckert *et al.* [23]. Its expression is:

$$V_{ev} = -\frac{D}{(1-C_p)} \left. \frac{\partial C}{\partial x} \right|_p \quad (15)$$

The mass fraction of water vapor corresponds to the saturation conditions explained by Dalton's law:

$$C_p = \frac{P_p M_v}{[P_p M_v + (P - P_p) M_a]} \quad (16)$$

$$-\lambda \left( \frac{\partial T}{\partial x} \right) - \rho L_v V_{ev} = -\lambda_s \left( \frac{T_{pe} - T_{pi}}{E} \right) = (h_R + h_C)(T_{amb} - T_{pe}) \quad (17)$$

The convective transfer coefficient  $h_C$  is correlated with the Rayleigh number ( $GrPr$ ) according to J. F Sacadura[24]:

$$h_C = Nu \lambda_{air} / H \quad (18)$$

$$Nu = a(GrPr)^m \quad (19)$$

$$\text{For: } 10^4 < GrPr < 10^9 ; a = 0.59 ; m = 0.25 \quad (20)$$

$$\text{For: } 10^9 < GrPr < 10^{13} ; a = 0.21 ; m = 0.4 \quad (21)$$

$$Gr = \frac{g \beta_T (T_{pe} - T_{amb}) H^3}{\vartheta_{air}^2} \quad (22)$$

$$h_R = \gamma \sigma (T_{pe}^2 + T_{amb}^2) (T_{pe} + T_{amb}) \quad (23)$$

The total heat flux exchanged between the wet wall and the flow is the sum of the sensible heat flux and the latent heat flux.

$$Q_T = Q_S + Q_L = \lambda \left. \frac{\partial T}{\partial x} \right|_p + \dot{m}''_C L_v \quad (24)$$

$$Nu_S = \frac{Dh}{\lambda} \frac{Q_S}{(T_p - T_b)} = \frac{Dh}{\lambda} \left. \frac{\partial T}{\partial x} \right|_p \quad (25)$$

$$Nu_L = \frac{Dh}{\lambda} \frac{Q_L}{(T_p - T_b)} = \frac{\dot{m}''_C L_v Dh}{\lambda (T_p - T_b)} \quad (26)$$

$$Sh = \frac{Dh}{(C_p - C_b)} \left. \frac{\partial C}{\partial x} \right|_p \quad (27)$$

$$Re = U_e Dh / \vartheta_e \quad (28)$$

$$Dh = 2R \quad (29)$$

$$Pr = \rho_e \vartheta_e C_{pe} / \lambda_e \quad (30)$$

$$Sc = \vartheta_e / D_e \quad (31)$$

## 2.2.5. DIMENSIONLESS EQUATIONS

The dimensionless equations and boundary conditions are obtained by dividing the various variables by the variables by the characteristic quantities of the system given in table 1.

**Table. 1. Dimensionless variables**

Designation	Dimensionless variable
Radial coordinate	$x^* = \frac{x}{Dh}$

Axial coordinate	$x^* = \frac{x}{Dh}$
Radial velocity	$V^* = \frac{U_e}{V}$
Temperature	$T^* = \frac{T}{T_e}$
Pressure	$P^* = \frac{P}{\rho_e U_e^2}$
Concentration	$C^* = \frac{C}{C_e}$
Density	$\rho^* = \frac{\rho}{\rho_e}$
Dynamic viscosity	$\vartheta^* = \frac{\vartheta}{\vartheta_e}$
Thermal conductivity	$\lambda^* = \frac{\lambda}{\lambda_e}$
Thermal diffusivity	$D^* = \frac{D}{D_e}$
Specific heat	$Cp^* = \frac{Cp}{Cp_e}$
Radius of channel	$R^* = \frac{R}{Dh}$
Height of channel	$H^* = \frac{H}{Dh}$
kinematic viscosity	$\mu^* = \frac{\mu}{\mu_e}$

❖ **The continuity equation**

$$\frac{\partial(\rho^* V^*)}{\partial x^*} + \frac{\partial(\rho^* U^*)}{\partial z^*} = 0 \quad (32)$$

❖ **The axial equation of momentum**

$$\rho^* \frac{\partial U^*}{\partial \tau} + \frac{\partial(\rho^* V^* U^*)}{\partial x^*} + \frac{\partial(\rho^* U^* U^*)}{\partial z^*} = -\frac{\partial P^*}{\partial z^*} + \frac{\partial}{\partial x^*} \left( \frac{\mu^*}{Re} \frac{\partial U^*}{\partial x^*} \right) + \frac{\partial}{\partial z^*} \left( \frac{\mu^*}{Re} \frac{\partial U^*}{\partial z^*} \right) \quad (33)$$

❖ **The radial equation of momentum**

$$\rho^* \frac{\partial V^*}{\partial \tau} + \frac{\partial(\rho^* V^* V^*)}{\partial x^*} + \frac{\partial(\rho^* U^* V^*)}{\partial z^*} = \frac{\partial}{\partial x^*} \left( \frac{\mu^*}{Re} \frac{\partial V^*}{\partial x^*} \right) + \frac{\partial}{\partial z^*} \left( \frac{\mu^*}{Re} \frac{\partial V^*}{\partial z^*} \right) \quad (34)$$

❖ **The energy conservation equation**

$$\rho^* C_p^* \frac{\partial T^*}{\partial \tau} + \frac{\partial(\rho^* C_p^* V^* T^*)}{\partial x^*} + \frac{\partial(\rho^* C_p^* U^* T^*)}{\partial z^*} = \frac{1}{Pr Re} \left[ \frac{\partial}{\partial x^*} \left( \lambda^* \frac{\partial T^*}{\partial x^*} \right) + \frac{\partial}{\partial z^*} \left( \lambda^* \frac{\partial T^*}{\partial z^*} \right) \right] \quad (35)$$

❖ **The water vapor diffusion equation**

$$\rho^* \frac{\partial C^*}{\partial \tau} + \frac{\partial(\rho^* V^* C^*)}{\partial x^*} + \frac{\partial(\rho^* U^* C^*)}{\partial z^*} = \frac{1}{Sc Re} \left[ \frac{\partial}{\partial x^*} \left( \rho^* D^* \frac{\partial C^*}{\partial x^*} \right) + \frac{\partial}{\partial z^*} \left( \rho^* D^* \frac{\partial C^*}{\partial z^*} \right) \right] \quad (36)$$

❖ **The flow rate conservation equation**

$$\int_0^{R^*} U^* dx^* = Q_{ev}^* + Q_e^* \quad (37)$$

### 2.2.6. INITIAL CONDITIONS

$$U^*(x^*, z^*) = 0; \quad V^*(x^*, z^*) = 0; \quad T^*(x^*, z^*) = 1; \quad C^*(x^*, z^*) = 1 \quad (38a-d)$$

### 2.2.7. BOUNDARY CONDITIONS

- At the channel entrance;  $z^* = 0; 0 \leq x^* \leq R^*$

$$U^*(x^*, z^*) = \frac{3}{2} \left[ 1 - \left( \frac{x^*}{R^*} \right)^2 \right] \quad (39)$$

$$V^*(x^*, z^*) = 0; \quad T^*(x^*, z^*) = 1; \quad C^*(x^*, z^*) = 1 \quad (40a-c)$$

- To the wall;  $x^* = R^*; 0 \leq z^* \leq H^*$

$$U^*(x^*, z^*) = 0; \quad V^*(x^*, z^*) = V_{ev}^* \quad (41)$$

$$V_{ev}^* = \frac{D}{DhU_e \left( \frac{1}{C_e - C_p^*} \right)} \frac{\partial C^*}{\partial x^*} \Big|_p \quad (42)$$

$$C_p^* = \frac{P_p^* - M_v^*}{P_p^* M_v^* + (P^* - P_p^*) M_a} \quad (43)$$

$$\lambda^* \left( \frac{\partial T^*}{\partial x^*} \right) + \frac{\rho^* L_V V_{ev} Dh}{\lambda_e T_e} = \lambda_S^* \left( \frac{T_{Pi}^* - T_{Pe}^*}{E^*} \right) = \frac{Dh}{\lambda_0} (h_R + h_C) (T_{Pe}^* - T_{amb}^*) \quad (44)$$

- At the axis of symmetry;  $x^* = 0; 0 \leq z^* \leq H^*$

$$\partial V^*(x^*, z^*) = 0 \quad (45)$$

$$\frac{\partial U^*(x^*, z^*)}{\partial x^*} = 0; \quad \frac{\partial T^*(x^*, z^*)}{\partial x^*} = 0; \quad \frac{\partial C^*(x^*, z^*)}{\partial x^*} = 0 \quad (46a-c)$$

- At the channel outlet;  $z^* = H^*; 0 \leq x^* \leq R^*$

$$\frac{\partial U^*(x^*, z^*)}{\partial z^*} = 0; \quad \frac{\partial V^*(x^*, z^*)}{\partial z^*} = 0; \quad \frac{\partial T^*(x^*, z^*)}{\partial z^*} = 0; \quad \frac{\partial C^*(x^*, z^*)}{\partial z^*} = 0 \quad (47a-d)$$

The Nusselt and Sherwood numbers become:

$$Nu_S = \frac{1}{(T_p^* - T_b^*)} \frac{\partial T^*}{\partial x^*} \Big|_p \quad (48)$$

$$Nu_L = \frac{m_C^L L_V Dh}{\lambda_e \lambda^* T_e (T_p^* - T_b^*)} \quad (49)$$

$$Sh = \frac{1}{(c_p^* - c_b^*)} \frac{\partial C^*}{\partial x^*} \Big|_p \quad (50)$$

## 2.3. NUMERICAL METHODOLOGY

The discretization of equations (32), (34), (35) and (36) by the finite volume method [17] leads to an algebraic equation system of N equations with N unknowns. Each equation

system obtained is tridiagonal and is therefore solved by Thomas' algorithm. As for equation (33), it leads to a system of N equations with (N+1) unknowns. For this, it is completed by equation (37) and then solved by the Gauss algorithm. The convergence criterion chosen is:

$$\frac{\phi^{k+1}(I,J) - \phi^k(I,J)}{\phi^{k+1}(I,J)} < 10^{-5} \quad (51)$$

In this expression, k represents the number of iterations and  $\Phi = T^*, C^*, U^*, V^*$ .

### 3. RESULTS AND DISCUSSION

The results are recorded when the regime stabilizes at a time  $t = 3500s$  and are presented in tabular, profile and iso-values form under the following conditions:  $T_{amb} = 298.15K$ ,  $T_e = 323.15K$  with Reynolds number between 500 and 1500.

#### 3.1. MODEL VALIDATION

To validate our numerical calculation code, we compared our numerical results with those of Othmane[25], for a stationary flow with mass transfer (see fig 2). The relative error resulting from comparison of the two results is of the order of 7%.

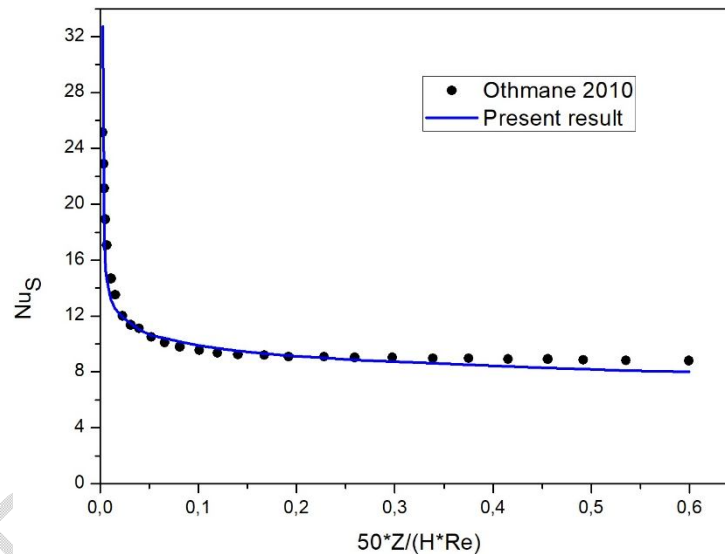


Fig. 2. Validation of the numerical code ( $T_o = 20^\circ C$ ,  $T_w = 40^\circ C$ ,  $\phi_o = 50\%$ ,  $Pr = 0.703$ ,  $Sc = 0.592$ ,  $Re = 400$ ).

#### 3.2. MESH SENSITIVITY STUDY

To ensure that our results are independent of the mesh, a mesh sensitivity study was carried out. This study showed that the mesh size (41x112), even quadrupled, did not significantly modify the sensitive Nusselt (see table 2). Consequently, the mesh (41x112) was retained for the rest of the study.

Table. 2. Grid independence

Grid( $X^*, Z^*$ )	$Z^*=20$	$Z^*=40$	$Z^*=60$	$Z^*=80$
	Values of $Nu_s$			
(41x112)	8,0186	6,5718	5,9367	5,5652
(82x224)	8,7732	6,8555	5,9899	5,4705

### 3.3. INFLUENCE OF REYNOLDS NUMBER ON THE DYNAMIC FLOW FIELD

Figure 3 shows the distribution of the flow velocity field for Reynolds numbers of 500, 1000 and 1500. We find a laminar flow for the three chosen Reynolds numbers. The above figures provide an overall view of the flow velocity gradient, which reveals higher velocities in the center of the channel and lower velocities when approaching the walls. The velocity of the flow increases with the number of Reynolds and this results in an improvement of the convective transfers. Indeed, the increase in inertia forces contributes to the decrease of the diffusive transport of the amount of motion. This decrease is also accompanied by that of the adhesion of the fluid to the wall.

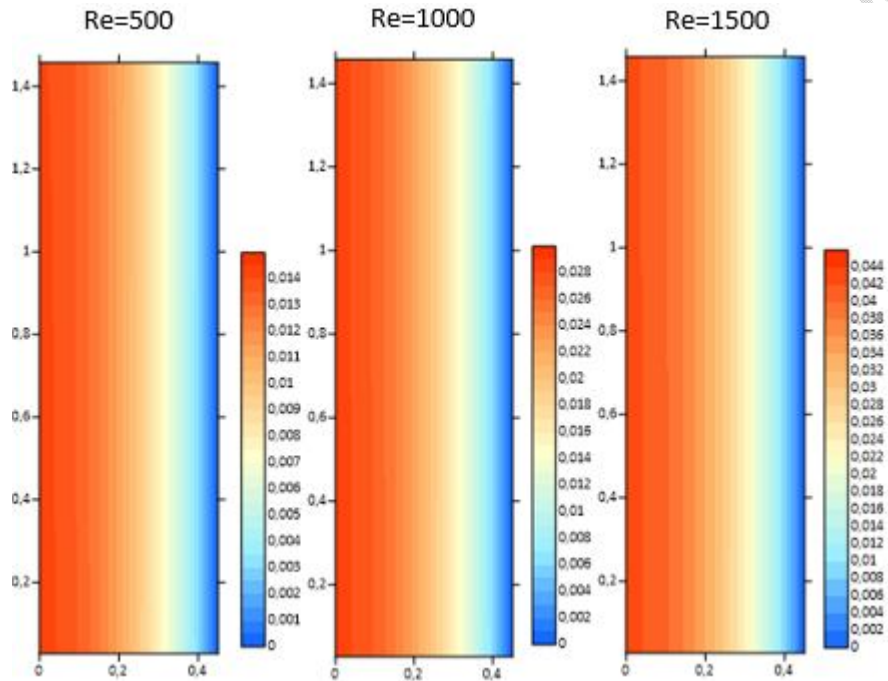
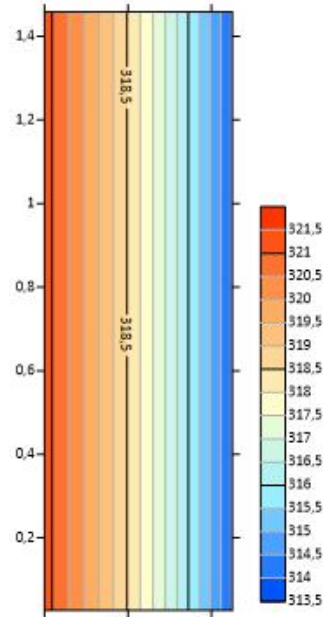


Fig.3. Velocity fields

### 3.4. INFLUENCE OF REYNOLDS NUMBER ON THE THERMAL FIELD

Figure 4 shows the thermal field distribution for a creeping flow with a Reynolds number of  $10^{-3}$ . The thermal field is uniformly distributed. The isothermal lines are parallel to each other and also in the direction of flow. Compared to the walls, temperature gradients show higher values in the center of the channel. The decrease in flow inertia is accompanied by an increase in viscous forces and thus the diffusive transport of the amount of movement.



**Fig.4. Thermal field for creep flow,  $Re=10^{-3}$**

Figure5 shows thermal fields for Reynolds numbers ranging from 500 to 1500. The contours of the isotherms show a profile of thermal gradients, with higher temperatures in the center of the channel. The isothermal lines narrow near the walls, indicating a zone of strong thermal gradients. Increased inertial forces enhance convective momentum transport. This in turn reduces the fluid's adhesion to the wall, and hence diffusive transfer.

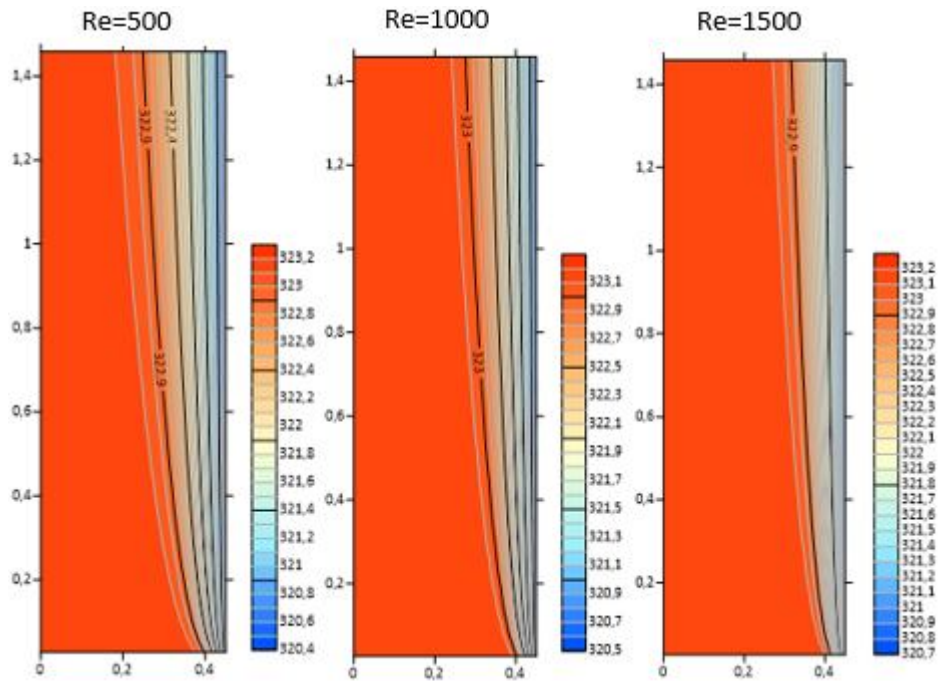


Fig.5. Thermal fields

### 3.5. INFLUENCE OF REYNOLDS NUMBER ON MASS FIELD

Figure 6 shows mass fields for three different Reynolds numbers (500, 1000 and 1500). The mass concentration iso-values show a distribution similar to that of the isotherms. The highest mass concentration values are found in the center of the channel. The similarity between mass and thermal distributions is explained by the Prandtl and Schmidt numbers, which are close for water vapor. The increase in Reynolds number is accompanied by the concentration of iso-concentration lines towards the walls.

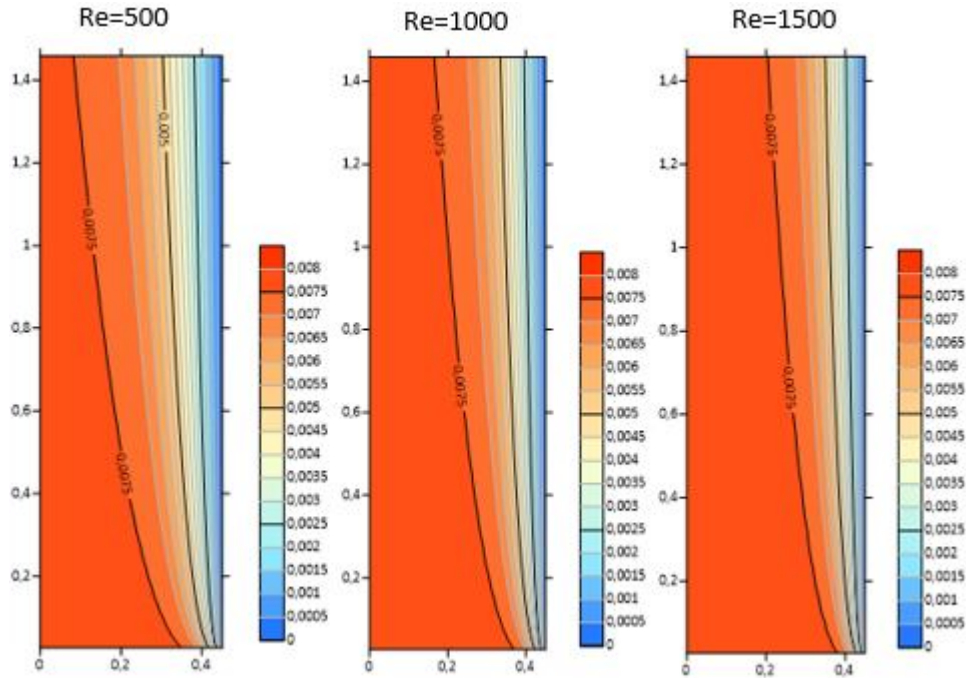


Fig. 6. Massfields

### 3.6. REYNOLDS NUMBER INFLUENCE ON HEAT TRANSFER

Figures (7-8) show the evolution of the latent and sensitive Nusselt numbers along the channel as a function of Reynolds number. It can be seen that the latent and sensitive Nusselt numbers show large values at the channel inlet and smaller values at the outlet. This is due to the steep thermal gradients at the leading edge of the channel. At the channel outlet, these gradients become small due to wall heating and the evacuation of the water vapor contained in the fluid. We also observe a gradual increase in these numbers as a function of Reynolds number. Indeed, increasing flow velocity leads to an increase in latent and sensible heat transfer, as condensation at the wall releases heat that is absorbed by the flow.

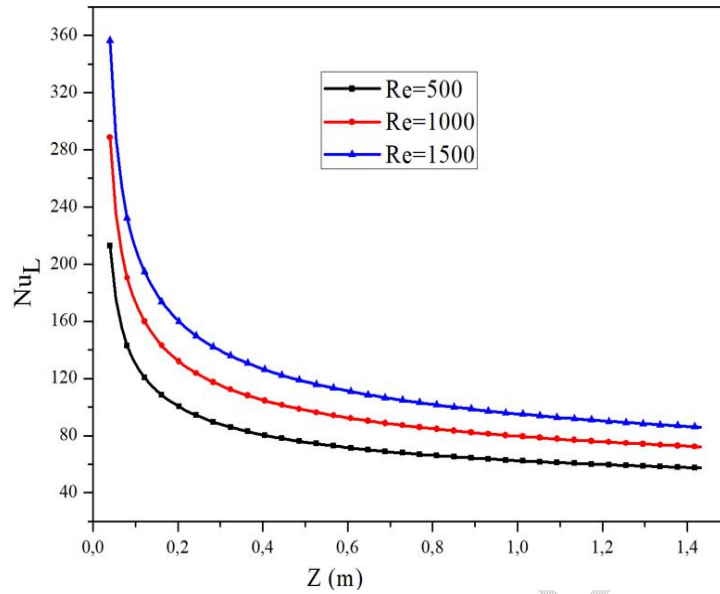


Fig. 7. Latent Nusselt number versus Reynolds number

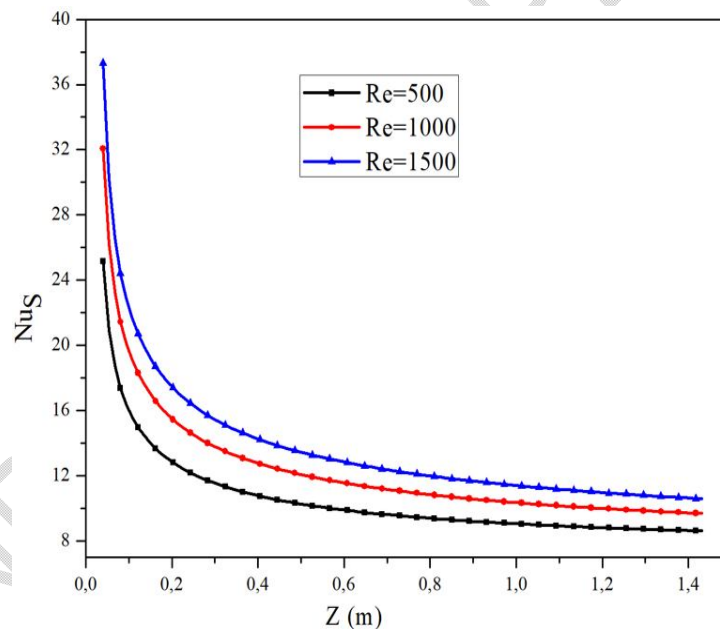
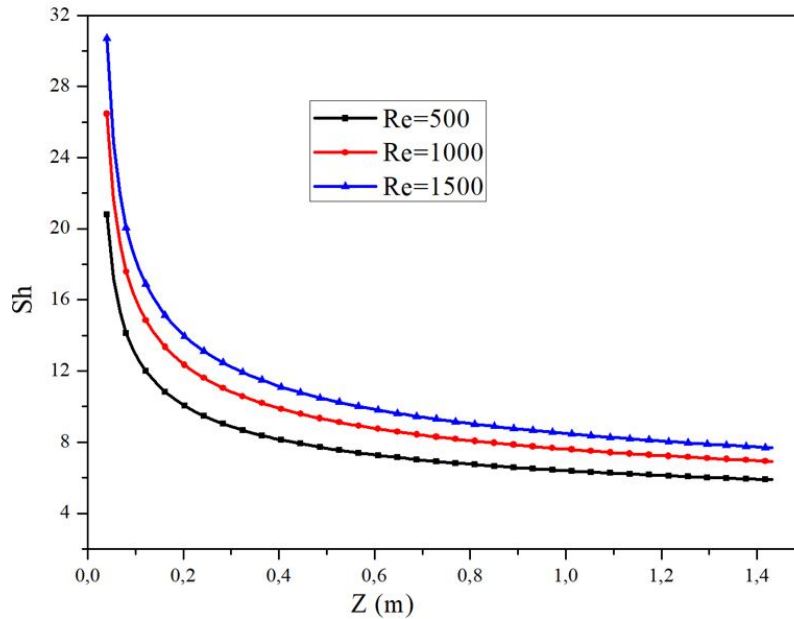


Fig. 8. Sensitive Nusselt number versus Reynolds number

### 3.7. REYNOLDS NUMBER INFLUENCE ON MASS TRANSFER

Figure 9 shows the evolution of the Sherwood number as a function of the Reynolds number. The shape of the Sherwood number is similar to that of the Nusselt number, since the Prandtl number and the Schmidt number are very close for water vapor. At the entrance to the channel, the Sherwood number takes on significant values and remains almost constant in the rest of the domain. This is because mass fraction gradients increase with flow acceleration, and are greater at the leading edge of the channel than at the outlet.



**Fig. 9. Sensitive Nusselt number versus Reynolds number**

#### 4. CONCLUSION

In this work, we carried out a numerical study of coupled heat and mass transfer in a vertical channel with wet walls, whose heat exchange with the outside environment is governed by natural convection and radiation. Forced laminar flow was modeled by the Navier-Stokes equations and the flow conservation equation. These equations were discretized using the finite volume method and then solved using the Thomas and Gauss algorithms. The effect of Reynolds number on heat and mass transfer was a particular focus of attention. Numerical simulation of velocity, temperature and mass fields was therefore carried out, considering Reynolds numbers of 500, 1000 and 1500 in addition to a so-called Stokes flow. The results show that an increase in Reynolds number leads to an increase in heat and mass transfer. This increase is greatest at the leading edge of the channel, with latent heat transport dominating throughout the channel.

#### NOMENCLATURES

A\*: Dimensionless value  
 T: Temperature (K)  
 H: Channel height (m)  
 R: Channel radius (m)  
 V: Radial velocity ( $\text{m}\cdot\text{s}^{-1}$ )  
 U: Axial velocity ( $\text{m}\cdot\text{s}^{-1}$ )  
 t: Time (s)  
 P: Pressure ( $\text{N}\cdot\text{m}^{-2}$ )  
 Cp: Thermal mass capacity ( $\text{J}\cdot\text{Kg}^{-1}\cdot\text{K}^{-1}$ )  
 Q: Flow rate ( $\text{m}^3\cdot\text{s}^{-1}$ )  
 D: Diffusion coefficient ( $\text{m}^2\cdot\text{s}^{-1}$ )  
 L: Latent heat ( $\text{J}\cdot\text{Kg}^{-1}$ )

E: Thickness (m)  
h: Heat transfer coefficient ( $\text{W}\cdot\text{m}^{-2}\cdot\text{K}^{-1}$ )  
M: Molar mass ( $\text{Kg}\cdot\text{mol}^{-1}$ )  
Gr: Grashof number  
Re: Reynolds number  
Nu: Nusselt number  
Sh: Sherwood number  
Pr: Prandtl number  
Sc: Schmidt number  
g: Accelerating gravity ( $\text{m}\cdot\text{s}^{-2}$ )  
 $\beta$ : Thermal expansion coefficient ( $\text{K}^{-1}$ )  
 $\vartheta$ : Kinematic viscosity ( $\text{m}^2\cdot\text{s}^{-1}$ )  
 $\mu$ : Dynamic viscosity ( $\text{Kg}\cdot\text{m}^{-1}\cdot\text{s}^{-1}$ )  
 $\sigma$ : Stefan Boltzmann's constant ( $\text{W}\cdot\text{m}^{-2}\cdot\text{K}^{-4}$ )  
Dh: Hydraulic diameter (m)  
 $\dot{m}''$ : Evaporated mass flow rate ( $\text{Kg}\cdot\text{s}^{-1}$ )  
 $\lambda$ : Thermal conductivity ( $\text{W}\cdot\text{m}^{-1}\cdot\text{K}^{-1}$ )  
 $\rho$ : Density ( $\text{Kg}\cdot\text{m}^{-3}$ )

#### **DISCLAIMER (ARTIFICIAL INTELLIGENCE)**

Author(s) hereby declare that NO generative AI technologies such as Large Language Models (ChatGPT, COPILOT, etc) and text-to-image generators have been used during writing or editing of manuscripts.

#### **REFERENCES**

1. Baragh, S., Shokouhmand, H., Ajarostaghi, S. S. M., Nikian, M. (2018). An experimental investigation on forced convection heat transfer of single-phase flow in a channel with different arrangements of porous media. *International Journal of Thermal Sciences*, 134, 370–379. <https://doi.org/10.1016/j.ijthermalsci.2018.04.030>.

2. Ikram, M. M., Saha, G., & Saha, S. C. (2021). Conjugate forced convection transient flow and heat transfer analysis in a hexagonal, partitioned, air filled cavity with dynamic modulator. *International Journal of Thermal Sciences*,167. <https://doi.org/10.1016/j.ijheatmasstransfer.2020.120786>.
3. Fanambinantsoa, V. H., Rakotomanga, F. A., & Randriazanamparany, M. A. (2016). Numerical study of forced convection in a horizontal rectangular channel with a sinusoidal protuberance. *Afrique Science*, 12(6)353–364. French.
4. Alsabery, A. I., Sidik, N. A. C., Hashim, I., & Muhammad, N. M. (2021). Impacts of two-phase nanofluid approach toward forced convection heat transfer within a 3D wavy horizontal channel. *Chinese Journal of Physics*, 77, 350–365. <https://doi.org/10.1016/j.cjph.2021.10.049>.
5. Oubella, M., Feddaoui, M., Mir, R. (2015). Numerical study of heat and mass transfer during evaporation of a thin liquid film. *Thermal Science*, 19(5), 1805–1819. <https://doi.org/10.2298/tsci130128145o>
6. Mechergui O. Numerical study of mass and heat transfers in natural convection in a channel: influence of the shape of the wall. Thesis University of Perpignan Via Domitia; France 2017. French.
7. Oulaid O, Benhamou B, Galanis N. Effect of the variability of thermo-physical properties on coupled heat and mass transfers in a vertical channel. 14th International Thermal Days. Tunisia 2009. French.
8. Karim, M. F., Islam, S., Rahman, M. M., Paul, A., & Mandal, G. (2024). A numerical investigation on forced convection heat and mass transfer performance in a right triangular cavity. *International journal of Thermofluids*, 21. 100578doi: 10.1016/j.ijft.2024.100578.<https://doi.org/10.1016/j.ijft.2024.100578>
9. Singh, A., Khan, I. A., Khan, M. Z., & Mahto, P. (2021). The effect of low Reynoldsnumber on coefficient of S-type pitot tube with the variation in port to port distance. *Materials Today : Proceedings*, 45, 7810–7815.<https://doi.org/10.1016/j.matpr.2020.12.174>.
10. Azizi, Y., Benhamou, B., Galanis, N.,& El-Ganaoui, M. (2007). Buoyancy effects on upward and downward laminar mixed convection heat and mass transfer in a vertical channel,*International Journal of Numerical Methods for Heat and Fluid Flow*, 17(3), 333–353, 2007, doi: <https://doi.org/10.1108/09615530710730193>.
11. Boukadida, N.,& Nasrallah, B. S.(2001). Mass and heat transfer during water evaporation in laminar flow inside a rectangular channel - Validity of heat and mass transfer analogy. *International journal ofthermal Science*, 40(1), 67–81. [https://doi.org/10.1016/S1290-0729\(00\)01181-9](https://doi.org/10.1016/S1290-0729(00)01181-9).
12. Helel, D.,&Boukadida, N. Heat and mass transfer in an unsaturated porous medium subjected to laminar forced convection, 13th International Thermal Days. France 2007.French.
13. Oulaid, O., Benhamou, B., &Galanis, N. (2010). Combined buoyancy effects of thermal and mass diffusion on laminar convection in a vertical isothermal channel. *Computational Thermal Sciences*, 2(2)125–138. <https://doi.org/10.1615/ComputThermalScien.v2.i2.30>.

14. Lin, T. F., Chang, J. Y., Yan, W. M. (1988). Analysis of combined buoyancy effects of thermal and mass diffusion on laminar forced convection heat transfer in a vertical tube. *Journal of heat transfer*, 110,337–344. <https://doi.org/10.1115/1.3250489>.
15. Yan, W., Ting, S., Soong, C. (1995). Convective heat and mass transfer along an inclined heated plate with film evaporation. *International journal of heat and mass transfer*, 38(7), 1261–1269.[doi:0017-9310\(94\)00241-X](https://doi.org/10.1017/9400241-X).
16. Mezaache, E., Daguene, M. (2004). Effects of inlet conditions on film evaporation along an inclined plate. *Solar energy*, 78, 535–542. <https://doi.org/10.1016/j.solener.2004.04.007>.
17. Cherif, A. S., Kassim, M. A., Benhamou, B., Harmand, S., Corriou, J. P., & Jabrallah, S. B. (2011). Experimental and numerical study of mixed convection heat and mass transfer in a vertical channel with film evaporation. *International Journal of Thermal Sciences*, 50(6), 942–953. <https://doi.org/10.1016/j.ijthermalsci.2011.01.002>.
18. Cherif, A. S., Kassim, M. A., Benhamou, B., Harmand, S., Corriou, J. P., & Jabrallah, S. B. (2011). Experimental and numerical study of mixed convection heat and mass transfer in a vertical channel with film evaporation. *International Journal of Thermal Sciences*, 50(6), 942–953. <https://doi.org/10.1016/j.ijthermalsci.2011.01.002>.
19. Turki, S., Abbassi, H., Nasrallah, S. B. (2003). Two-dimensional laminar fluid flow and heat transfer in a channel with a built-in heated square cylinder. *International Journal of Thermal Sciences*, 42, 1105–1113. [https://doi.org/10.1016/S1290-0729\(03\)00091-7](https://doi.org/10.1016/S1290-0729(03)00091-7).
20. Zermane, S., Boudebous, S., Boukroune, N. (2005). Numerical study of laminar mixed convection in ventilated cavities. *Science & Technology*, 23, 34–44.
21. Diallo DM. Mathematical modeling and numerical simulation of hydrodynamics: case of flooding downstream of the Diama dam. Thesis; University of Franche-Comté, 2010. France. French.
22. Feddaoui, M., Mir, A., Belahmidi, E. (2023). Cocurrent turbulent mixed convection heat and mass transfer in falling film of water inside a vertical heated tube. *International Journal of Heat and Mass Transfer*, 46(18), 3497–3509. [https://doi.org/10.1016/S0017-9310\(03\)00129-7](https://doi.org/10.1016/S0017-9310(03)00129-7).
23. Eckert ER, Drake R. Analysis of heat and mass transfer. 1972. New York.
24. Sacadura JF. Thermal transfers: initiation and deepening. 2015;625–691. ISBN: 978-2-7430-1993-8. Lavoisire. Paris. French.
25. Oulaid O. Coupled transfer of heat and mass by mixed convection with phase change in a channel. Thesis 2010. University of Sherbrooke, Canada. French.